ENGINEERING JOURNAL

Article

Morphology-Controlled Synthesis of Zeolite L and Physicochemical Properties

Wilaiporn Insuwan* and Kunwadee Rangsriwatananon

School of Chemistry, Institute of Science, Suranaree University of Technology, Nakhonratchasima 30000, Thailand
E-mail: wi_insuwan@hotmail.com*

Abstract. Zeolite L is a crystalline aluminosilicate compound and a typical chemical composition of $K_9Al_9Si_{27}O_{72}•nH_2O$ (n = 0–36). The structure and chemical properties, as well as their sizes and morphologies of zeolite L has led to various applications in different fields. The aim of this study is to investigate the effects of chemical compositions of the starting gel on the synthesis, size and morphology of zeolite L crystals. Zeolite L had been synthesized hydrothermally at 180 °C for 2 days, from gels with the molar compositions of 2.62-3.78 K_2O: 0.8-1.4 Al_2O_3: 8-12 SiO_2: 80-200 H_2O. The variation of chemical compositions led to the differences in morphologies and crystal sizes. Their morphologies varied from ice hockey to cylindrical shapes and their crystal sizes varying from 1.50-7.53 μm. With an increase in H_2O and SiO_2, the crystal size was also increased but decreased with an increase in K_2O. In varying Al_2O_3, there was no effect on their shapes which were still cylindrical but with different crystal sizes. Moreover, the adsorption of ethylene on zeolite L samples depended significantly on crystal shapes and sizes.

Keywords: Synthesis, zeolite L, morphology, ethylene adsorption.

ENGINEERING JOURNAL Volume 16 Issue 3
Received 14 November 2011
Accepted 17 January 2012
Published 1 July 2012
Online at http://www.engj.org/
DOI:10.4186/ej.2012.16.3.1

This paper is based on the oral presentation at the German-Thai Symposium on Nanoscience and Nanotechnology 2011—Green Nanotechnology of the Future, GTSNN 2011, in Nakhon Ratchasima, Thailand, 13-16 September 2011.

DOI:10.4186/ej.2012.16.3.1

1. Introduction

Zeolite L with well-defined size and morphology can be applied in various applications. Zeolite L was first described in 1968 [1]. It is hexagonal with unit cell dimensions of a = 18.4 Å and c = 7.5 Å and with space group P6/mmm. The typical chemical composition of zeolite L is $K_9[(AlO_2)_9(SiO_2)_{27}]\cdot 22H_2O$ [2]. Zeolite L is usually formed with the ratio of Si/Al between 3 and 6, but it is possible to make low-silica LTL phases with Si/Al equal 1 [3]. Preparations of the zeolite L have been reported by various investigators. Most of the reports on the synthesis of zeolite L are involved with an increase in SiO_2 and H_2O and decrease in KOH and $Al(OH)_3$ leading to an increase in the size of zeolite L [4]. Recently, Yun-Jo Lee *et al.* [5] found when $Al_2(SO_4)_3$ was used as alumina source instead of $Al(OH)_3$, the size of crystals increased with an increase in $Al_2(SO_4)_3$. Moreover, S. D. Bhat *et al.* [6] reported systematic studies of hydrothermal crystallization of K-LTL zeolite L at high temperature. The results showed that most of siliceous gel systems caused high rates of nucleation and crystallization. It resulted in the formation of more siliceous K-LTL zeolite L with less yield and clam shape agglomerates. In more aluminous system, the particle size, Si/Al ratio and the yield of product were found to be increased with a decrease in molar K_2O/SiO_2 ratio. Moreover, zeolite L crystals that are clam and hockey-puck have been synthesized [7]. When alkanolamine is added into starting sols, it led to clam shape [8]. In addition Larlur *et al.* [9] reported the synthesis of columnar/cylindrical shape of zeolite L to observe optical properties of dye loaded zeolite L. The structural and chemical properties of zeolite L, as well as their sizes and morphologies play a significant role in the applications. For large crystals (1-3 μm) with cylindrical shapes [8], they are useful for studying the optical and photophysical properties of dye-composites on single crystals by means of optical microscopy method. A disc-shaped morphology is an important prerequisite for the preparation of oriented monolayer of zeolite L on the substrate use for optimizing the utilization of dye-zeolite composites as photonic antenna system. Small crystals (30-50 nm) are useful for photonic antenna materials [10]. Recently, S. Trakarnroek *et al.* [11] studied the effects of catalyst prepared by loading Pt on different morphologies and channel lengths of the KL zeolite on the reaction of n-octane aromatization. They found that KL zeolite with cylindrical shape was an effective catalyst and the effectiveness strongly depended on the channel length of the zeolite L crystals. Moreover, zeolites are used as adsorbent for adsorption of ethylene and other gases [12]. The important role of ethylene is to control the growth process associated with aging of plants. Ethylene causes many physical changes in the appearance of fruits and vegetables such as colour change in fruits and stem wilting in flowers. Many researchers were trying to search for appropriate adsorbents for ethylene removal. Zeolites have been reported for ethylene adsorption [13, 14]. The ethylene adsorption isotherm of zeolite Y and modified zeolite Y by cationic surfactant were studied. The results shown that zeolite Y modified by PTAB can enhance the ethylene adsorption capacity up to 111.19 cm^3g^{-1} [15]. 13X zeolite could be also separated ethylene from CO_2 [16]. Many studies reported there are two types of interaction between ethylene and zeolite framework. Firstly, the filled ethylene π- orbital donates electron density into an empty metal σ –orbital which is called σ -donation. Secondly, d–π* back- donation is interaction between the empty antibonding (π*) molecular orbital of ethylene accepts electron density from the filled metal d-orbital. Sometime called all of interactions are cation– π interaction [15, 17, 18].

Although the amount of detail in the literature describing synthesis routes of zeolite L, but no reports on extensive range to control the crystal morphology of zeolite L have been reported so far. The morphology of the zeolite L crystals synthesized in this study range from ice hockey to cylindrical morphologies. The optimum conditions for synthesis zeolite L with different shapes under variation of several synthesis parameters (alkalinity, dilution, Al_2O_3 and SiO_2 content) and some physicochemical properties were studies.

2. Experimental Section

2.1. Materials and Chemicals

Colloidal silica sol (Ludox HS–40 from Dupont, 40% SiO_2) and aluminium hydroxide (CARLO ERBA, 98%) were used as silica and alumina sources, respectively. Potassium hydroxide (CARLO ERBA, 85%) was used for alkali metal cations. Ethylene gas with 99 % purity obtained from Mox (Malaysia) were selected as adsorbates on zeolite L.

2.2. Synthesis

Cylindrical shape: 2.62 K_20:Al_2O_3:10SiO_2:160H_2O Zeolite L crystals was synthesized by a method modified from the literature [19]. Weight of 0.59g of aluminium hydroxide was dissolved by boiling potassium hydroxide solution (1.28g of potassium hydroxide was added to 2.51g of double distillate water until clear solution. This solution was added to 5.52g of Ludox HS-40 with 4.82g of double distillate water in mixer. The clear solution mixture was stirred for 3 minutes to obtain gel with viscosity and turbidity. The starting gel was then transferred into a Teflon-lined autoclave for crystallization at 180 ˚C for 2 days without stirring. After crystallization, the Teflon-lined autoclave was cooled in cold water before opening. The product was washed with distilled water until the pH of liquid was close to 7. Finally, the crystalline solid was dried for overnight at 80 ˚C in an air oven. For another sample can be prepared by vary composition of starting materials.

2.3. Characterization

The products were analyzed by powder X-ray diffraction (XRD) using a Model D5005, Bruker, CuKα radiations scanning from 3-50˚ at a rate of 0.05 ˚/s with current 35 mV and 35 mA. The experimental XRD patterns of obtained products were compared with calculated ones reported in the collection of simulated XRD patterns [20]. To calculate crystallinity of zeolite L, the areas of main peaks located at 2θ = 5.5, 19.4, 22.7, 28.0, 29.1 and 30.7 were integrated. The chemical compositions were analyzed by energy dispersive XRF (EDS Oxford Instrument ED 2000) with Rh x-ray tube as a target with a vacuum medium. Scanning electron microscope (Model JSM6400, JEOL) at an acceleration voltage of 10-20 kV was used for the examination of zeolite L morphology. The framework was also confirmed by FT-IR (Spectrum GX, Perkin-Elmer) with KBr pellet technique in the range between 4000 and 400 cm^{-1}. The particle size distribution was determined by DPSA (Malvern Instrument, Masterizer 2000) with the sample dispersed in distilled water and analyzed by He-Ne laser. The specific surface area was evaluated by the nitrogen gas adsorption at -196 ˚C using automated volumetric equipment (Autosorb 1-Quantachrome Instrument, U.S.A).

2.4. Ethylene Adsorption

The determination of ethylene (C_2H_4) adsorption capability, the adsorption isotherm was carried out by NOVA 1200e instrument (Quantachrome Instrument, U.S.A) at adsorbate temperature of 0 ˚C.

3. Results and Discussion

3.1. XRD and FTIR

Figure 1 shows the XRD patterns of zeolite L with different morphologies. The patterns were compared to a standard pattern of commercial zeolite L (Union Carbide or UOP) [20]. The XRD pattern all of samples shows the same 2 theta (2θ) that the main peaks located at 2θ = 5.5, 19.4, 22.7, 28.0, 29.1 and 30.7. IR spectra of zeolite L crystals with different morphologies were shown in Fig. 2. The stretching vibration at 3480 - 3450 cm^{-1} which appeared in all the samples were attributed to the formation of H-bonds in water and one at 1641-1637 cm^{-1} was the bending vibration of water. The triplet band in the range 1098 - 1020 cm^{-1} corresponded to the previous report [21] indicating the internal vibrations of T-O-T (T = Si, Al)

tetrahedral. A sharp band around 767 - 772 cm^{-1} was the main band characteristics of external or internal symmetric stretching and the band around 608 - 611 cm^{-1} was the band characteristics of double-six-ring vibration. The bands at 478 - 482 cm^{-1} assigned to the T-O bending mode and a shoulder located at 432 cm^{-1} was the characteristics of a pore opening of external linkages. The band positions of internal and external T-O-T (T= Si, Al) tetrahedral vibration as well as double-six-ring vibration were observed to shift to higher wave numbers with an increase in Si/Al ratio of zeolite L. The trends agreed well with the report of [22].

3.2. Effects of KOH

Figure 3 shows the SEM photographs of the zeolite L samples. They were prepared from synthesis gels with the molar compositions of **a**K_2O:Al_2O_3:10SiO_2:160H_2O, where a = 2.62 (a), 2.78 (b), 3.04 (c), 3.26 (d), 3.54 (e) and 3.78 (f), to monitor the effects of KOH on the crystal morphology. K_2O had a high significant effect on the shape and crystal size of zeolite L (see Table 1). At low potassium oxide (2.62 mole), the shape of zeolite L crystal was cylindrical and the size 7.53 μm, while ice hockey shapes with 2.47-2.53 μm sizes occurred with K_2O varied from 2.78-3.26 moles. The clam-shape crystals with 2.17 and 1.58 μm sizes were observed at high concentration of KOH (3.54 and 3.78 moles of K_2O). It may arise from more dissolution of silica colloid according to more concentration of KOH. And also the polycondensation of hydroxoaluminate and silicate species was restricted [6]. Consequently, it provided coin-like-shape crystals apparently for high concentration of KOH and cylindrical shape for low concentration. Similar results of crystal sizes of zeolite L depending on alkaline concentration have also been found from various zeolites such as FAU, MFI, MCM-22 zeolite [23].

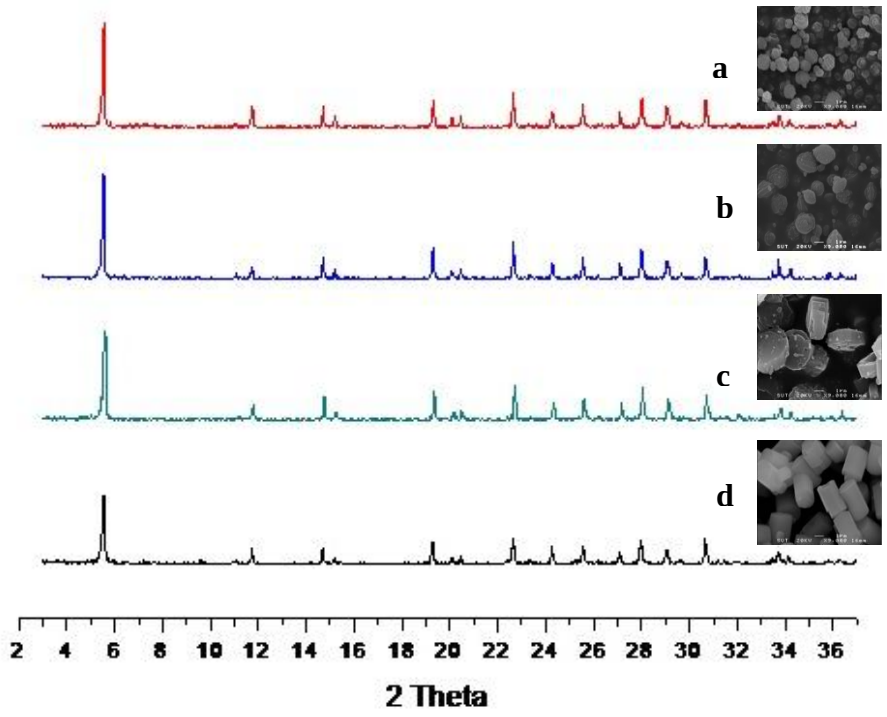

Fig. 1. XRD patterns of crystalline zeolite L with different morphologies, where (a) ice hockey shape; (b) clam shape; (c) disk shape; (d) cylindrical shape.

DOI:10.4186/ej.2012.16.3.1

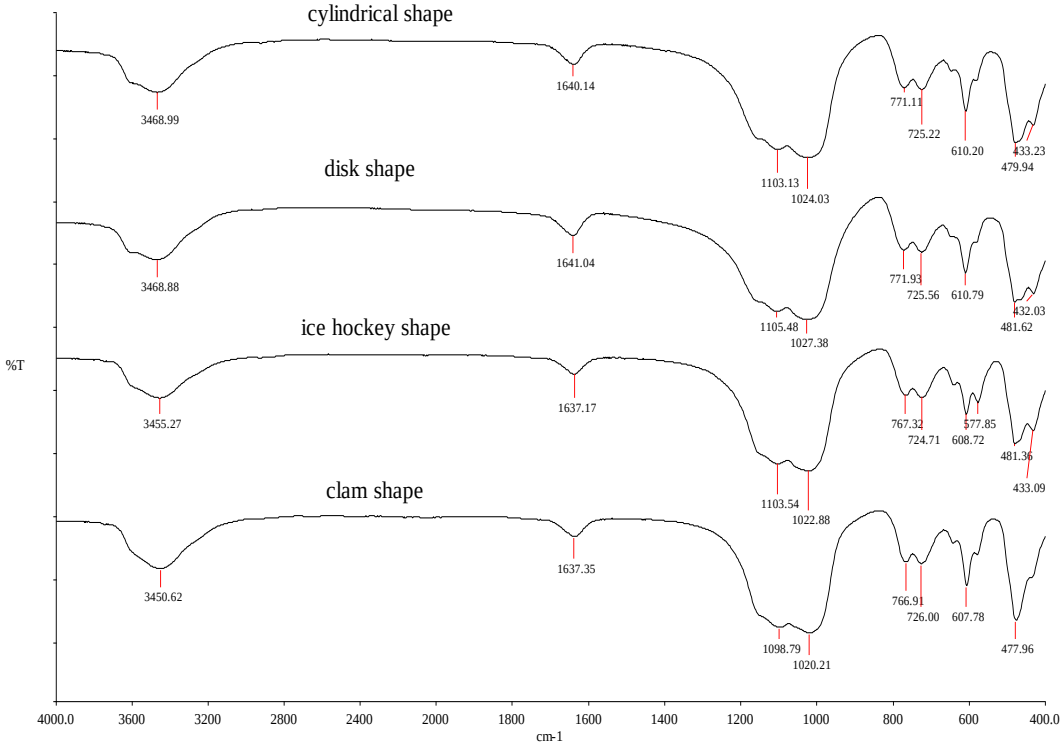

Fig. 2. IR spectra of zeolite L crystals with different morphologies.

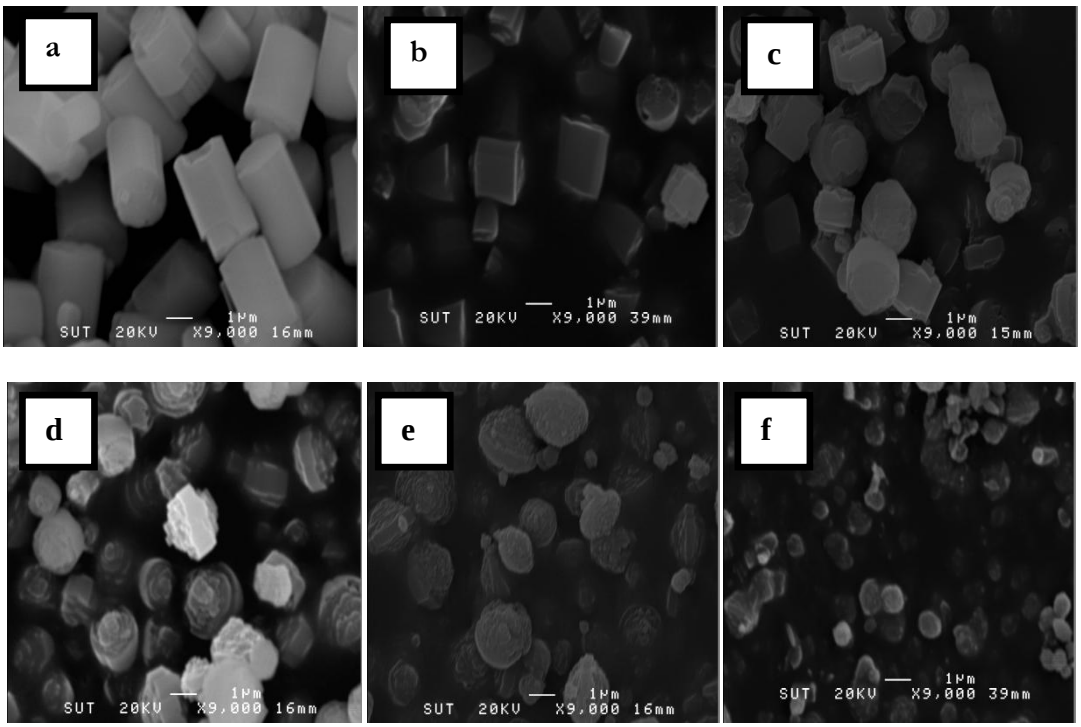

Fig. 3. SEM images of zeolite L crystals synthesized from the gel compositions **a**K_2O:Al_2O_3:10SiO_2:160H_2O, where a = 2.62 (a), 2.78 (b), 3.04 (c), 3.26 (d), 3.54 (e), 3.78 (f).

DOI:10.4186/ej.2012.16.3.1

3.3. Effects of Al_2O_3

Figure 4 shows the SEM image of the zeolite L samples prepared under variation of aluminum contents. The synthesis gels with the molar compositions of 2.62 K_2O: **b**Al_2O_3: 10SiO_2: 160H_2O, where b= 0.8 (a), 1.0 (b), 1.2 (c) and 1.4 (d), were monitored. Under this studied conditions, only cylindrical shape of all zeolite L morphologies was found. At 0.8 and 1.4 moles of Al_2O_3, the obtained solid contained only some crystalline phase but high amount of amorphous phase. (Two small additional pictures in Figs. 4(a) and 4(d) demonstrate crystalline phase of zeolite L). While at 1.0 and 1.2 moles, it was only a pure crystalline phase of zeolite L with a cylindrical shape 7.53 μm and 6.50 μm, respectively. The channel length was decreased with an increase in $Al(OH)_3$ (see Table 1).

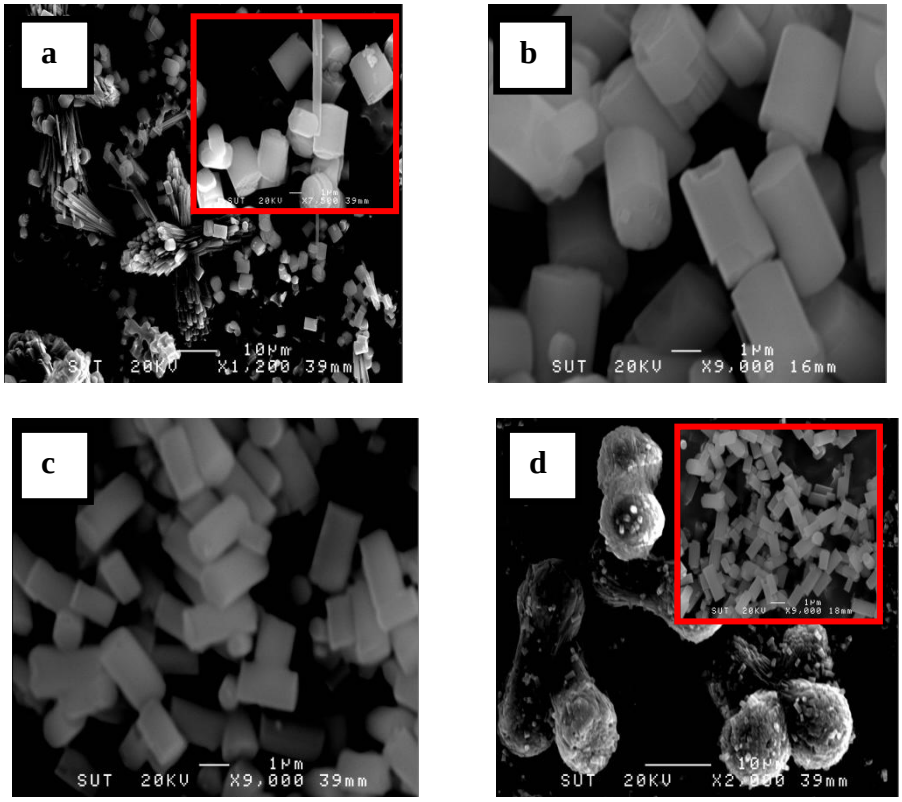

Fig. 4. SEM images of zeolite L crystals synthesized from the gel compositions 2.62K_2O:**b**Al_2O_3:10SiO_2:160H_2O, where b= 0.8 (a), 1.0 (b), 1.2 (c), 1.4 (d).

This was consistent with the report of Y. C. Kim *et al.* [24]. As the Al_2O_3 increased, the crystal size was decreased. This implies that the nucleation was enhanced due to the increase of Al_2O_3 and the incorporation of Al into tetrahedrally coordinated silicate framework which should have been enhanced. Our result showed that there is no effect of Al_2O_3 content on the morphology of zeolite L. The crystals maintained the cylindrical morphology, regardless of the size. Contrary to some reports, Al_2O_3 content has a great effect on the morphology and crystal size of crystals. They found that as the Al_2O_3 content was increased the crystallization time increased and the crystal size decreased due to the disruptive effect of the Al on the structure. In addition at low Al content, the crystal shape was round and an increase in Al content the crystals were changed to an elliptical rice-like morphology [5, 9, 25].

3.4. Effects of SiO_2

Figure 5 shows the SEM images of the zeolite L crystals from the synthesis gels with the molar compositions of 2.62 K_2O: Al_2O_3: **c**SiO_2: 160H_2O, where c = 8 (a), 9 (b), 10 (c) and 12 (d). At 8, 9 and 10 moles of SiO_2, only pure phase of zeolite L crystals appeared in an ice hockey (1.50 μm) and cylindrical shapes with 7.53 and 6.50 μm. In case of 12 moles of SiO_2, the yield contained a quite small amount of crystalline zeolite L. When SiO_2 content was too high (more than 12 moles) or too low (less than 8 moles),

the obtained solid appeared only in an amorphous phase. The average crystal size of zeolite L was increased from 1.50 to 7.53 μm with an increase in the concentration of SiO_2 from 8 to 10, respectively. It is consistent with Y. S. Ko and W. S. Ahn [4]. They found that the SiO_2/Al_2O_2 ratios of the synthesis mixture affected the shapes and sizes of the zeolite L crystals. The crystals were clam-shaped whereas the siliceous gel produced crystals having basal planes of more flatness. And also the crystal size was increased with an increase in SiO_2 content [26, 27].

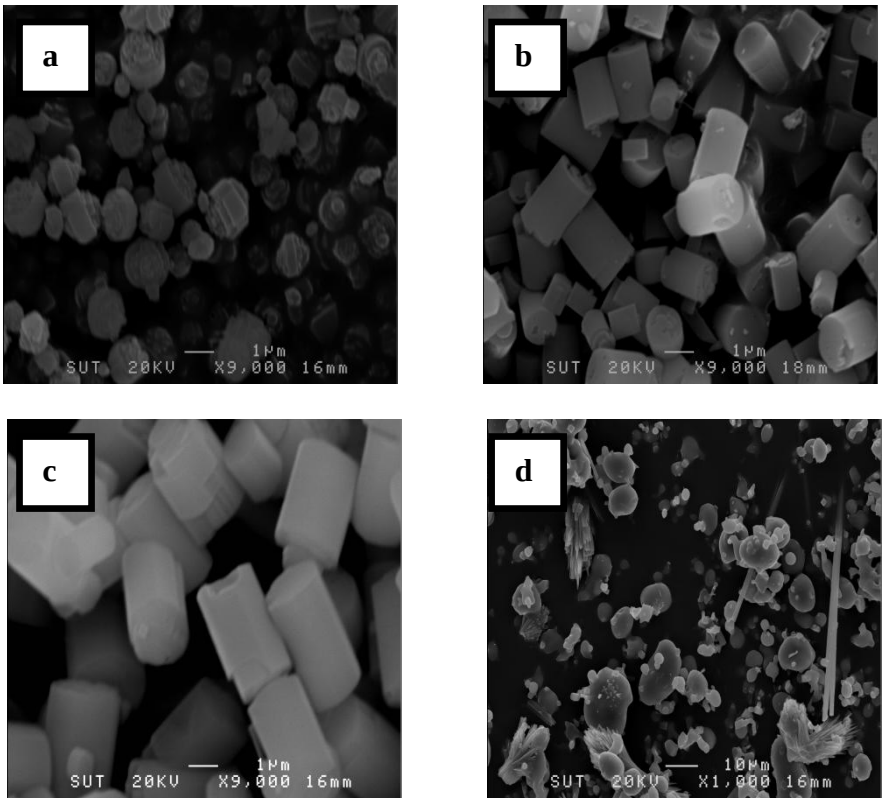

Fig. 5. SEM images of zeolite L crystals synthesized from the gel compositions $2.62K_2O:Al_2O_3:\mathbf{c}SiO_2:160H_2O$, where c = 8 (a), 9 (b), 10 (c), 12 (d).

3.5. Effects of H_2O

Figure 6 shows the SEM photographs of the synthesized zeolite L prepared from the synthesis gels with the molar compositions of 2.62 K_2O: Al_2O_3: 10SiO_2: **d**H_2O, where d = 80 (a), 100 (b), 160 (c), 180 (d) and 200 (e). At H_2O content of 80 and 100 moles, there were only pure zeolite L phases with a round and disk shape, respectively. Moreover, with H_2O of 160 mole the zeolite L crystal with a long cylindrical shape (7.53 μm) was observed. In case of H_2O contents varied from 180 to 200 moles, the mixed phases of zeolite L and zeolite W were appeared. (Two small additional pictures in Figs. 6(d) and 6(e) show the crystalline phase of zeolite L). Additionally, when the reaction time was extended to 3 days, in case of 180 and 200 moles of H_2O, at 180 moles, the obtained solid contained only single phase zeolite L. In contrast with 200 moles, mixed solid phases of zeolite L and zeolite W were still appeared. It was also found that the average crystal size of zeolite L increased as the H_2O increased. This may be attributed to the slowdown of nucleation and crystallization. The result agreed with the report of Y. C. Kim *et al.* [24]. If the water content in the optimum composition increased to 160 moles, the long cylindrical shape of zeolite L crystal was obtained. It indicated that in dilute systems a preferential growth along the c- direction was over the a-b plane. This was consistent with the report of Rhea Brent *et al.* [28]. The summary of the starting gel compositions in the synthesis of zeolite L and the products with some properties under the conditions studied was shown in Table 1.

DOI:10.4186/ej.2012.16.3.1

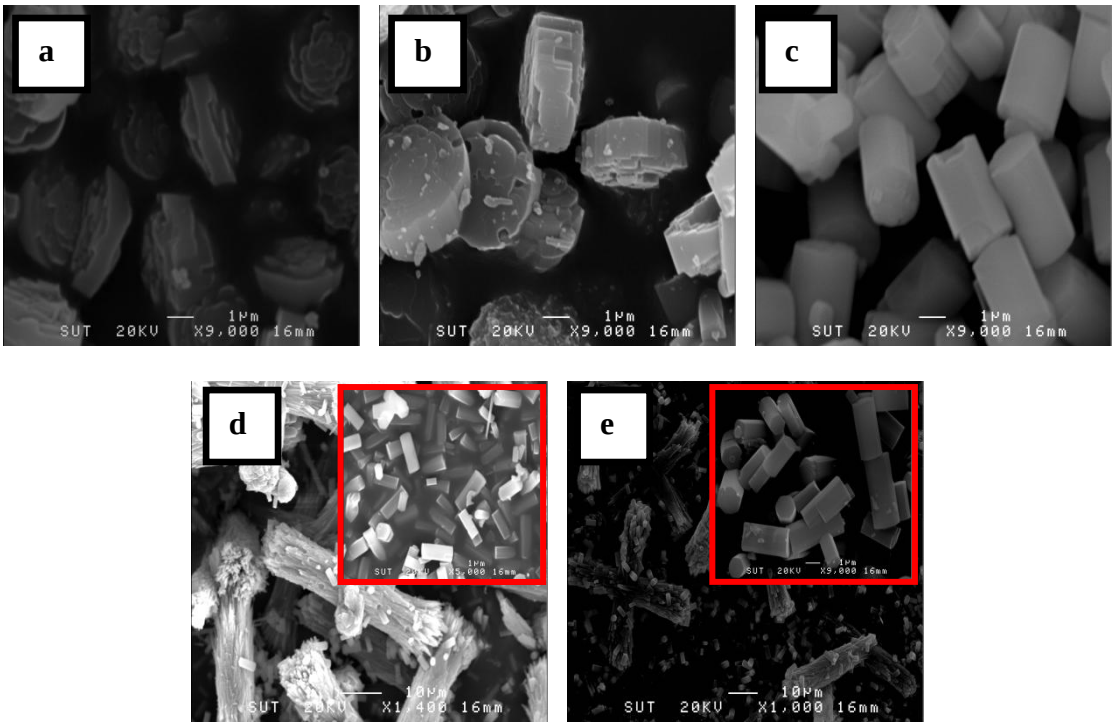

Fig. 6. SEM images of zeolite L crystals synthesized from the gel compositions $2.62K_2O:Al_2O_3:10SiO_2:\mathbf{d}H_2O$, where d = 80 (a), 100 (b), 160 (c), 180 (d), 200 (e).

3.6. Particle Size Distribution

Figure 7(a) shows particle size distribution of highly crystalline phase of zeolite L. For clam, ice hockey and round shapes (samples 5, 11 and 15 in Table 1, respectively), monomodal narrow sized distributions having an average particle size 2.17, 1.50 and 4.39 μm, respectively, were displayed. For cylindrical shape (samples 9), it showed a broad band distribution an average particle size 7.53 μm. Figure 7(b) shows the particle size distribution of the yield from the gel composition of $2.62K_2O:Al_2O_3:10SiO_2:180H_2O$ (see Table 1) under 2 days reaction time (sample 17) and 3 days (sample 18). For the 2 days reaction time, the particle size distribution existed more than one mode and was very wide due to an inhomogeneous of large particle sizes (see also Fig. 4(d)), while the 3 days reaction time, a shape distribution curve was shown due to the high crystalline content of zeolite L.

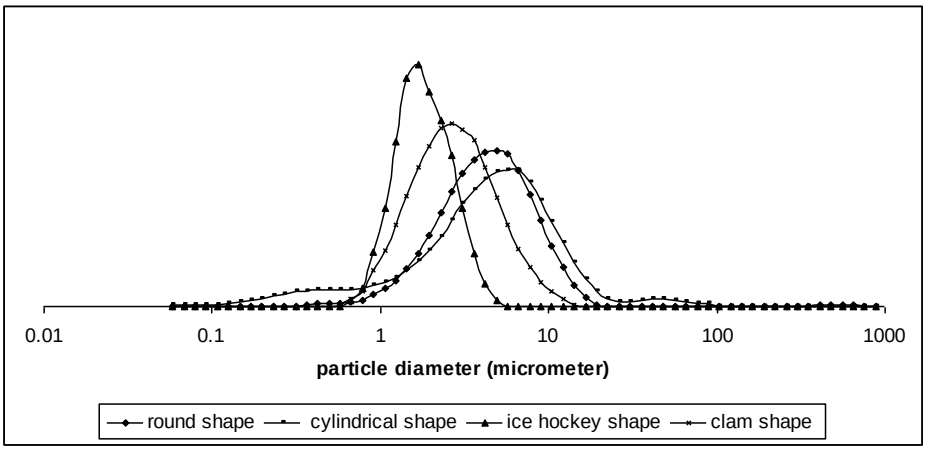

(a)

Fig. 7(a). Particle size distribution of zeolite L with different crystal shapes.

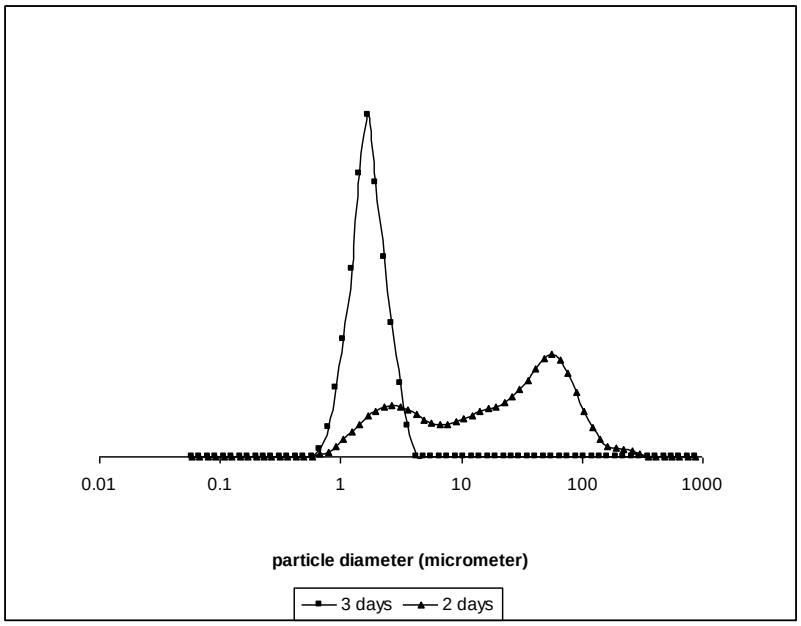

(b)

Fig. 7(b). Particle size distribution of obtained solid from gel molar composition of $2.62K_2O:Al_2O_3:10SiO_2:180H_2O$ at reaction time 2 days and 3 days.

Table 1. Summary of the chemical compositions of starting gel for synthesis of zeolite L and the obtained solid samples with their some properties under reaction time 2 days and at 180 ºC.

Sample	Chemical composition $K_2O:Al_2O_3:SiO_2:H_2O$	% Crystallinity of zeolite L **	Average particle size (μm)[a]	Morphology
1	**2.62**:1.00:10.00:160.00	78.90	7.53	Long cylindrical
2	**2.78**:1.00:10.00:160.00	98.30	2.49	Ice hockey
3	**3.04**:1.00:10.00:160.00	100.00	2.47	Ice hockey
4	**3.26**:1.00:10.00:160.00	92.30	2.53	Ice hockey
5	**3.54**:1.00:10.00:160.00	98.20	2.17	Clam
6	**3.78**:1.00:10.00:160.00	76.00	1.58	Clam
7	2.62:**0.80**:10.00:160.00	45.30	15.04	Cylindrical
8	2.62:**1.00**:10.00:160.00	91.70	7.62	Long cylindrical
9	2.62:**1.20**:10.00:160.00	100.00	6.50	Short cylindrical
10	2.62:**1.40**:10.00:160.00	32.70	13.50	Cylindrical
11	2.62:1.00: **8.00**:160.00	100.00	1.50	Ice hockey
12	2.62:1.00: **9.00**:160.00	n.	3.39	Short cylindrical
13	2.62:1.00:**10.00**:160.00	87.40	7.62	Long cylindrical
14	2.62:1.00:10.00: **80.00**	100.00	4.25	Round
15	2.62:1.00:10.00:**100.00**	79.20	4.39	Disk
16	2.62:1.00:10.00:**160.00**	79.00	7.53	Long cylindrical
17	2.62:1.00:10.00:**180.00**	n.	20.97	Cylindrical
18	2.62:1.00:10.00:**180.00***	n.	1.56	Ice hockey
19	2.62:1.00:10.00:**200.00**	n.	22.28	Cylindrical
20	2.62:1.00:10.00:**200.00***	n.	11.26	Cylindrical

* *Reaction time for 3 days.*

** *The Percentage of crystallinity was calculated by use of percent relative intensity obtained from integrated XRD pattern of the major peaks at 2θ = 5.5, 9.4, 22.7, 28.0, 29.1 and 30.*

[a] *Average particle size was evaluated by measuring at 50 % size on the cumulative distribution and n = not detect.*

DOI:10.4186/ej.2012.16.3.1

3.7. Adsorption of Ethylene on Zeolite L

The adsorption isotherms of ethylene on zeolite L with differences in sizes and shapes of the crystals were shown in Fig. 8.

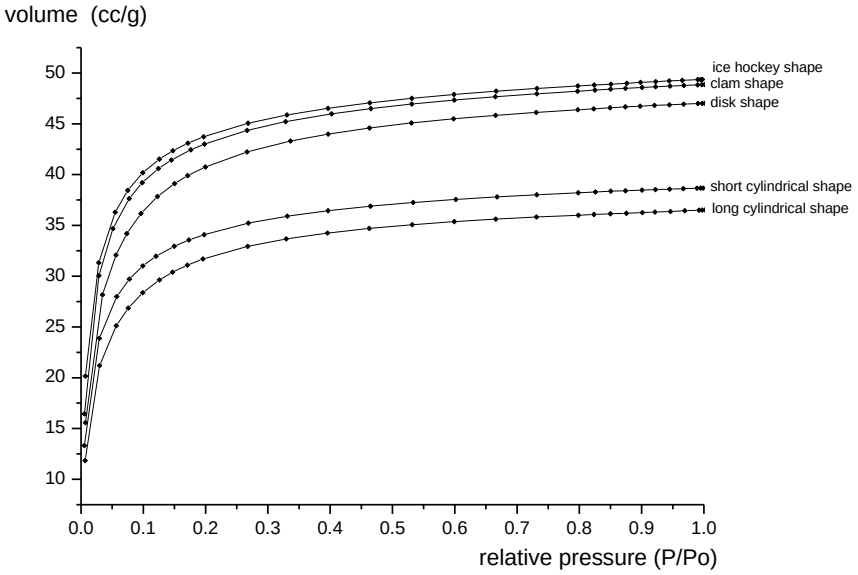

Fig. 8. Adsorption of ethylene on zeolite L crystals with different morphologies.

All of the adsorption isotherms exhibited a type I adsorption isotherm based on the IUPAC classification. The adsorption isotherms of the samples were divided into two groups. The first group (ice hockey, clam and disk shape with crystal sizes: 1.50, 2.17, and 4.39 μm, respectively) had a relatively higher adsorptive capability than that of the other group (cylindrical with 6.50 μm and 7.53 μm). It could be attributed to the fact that the smaller the crystal size was, the more the surface areas became (see Table 2). When considered the effect of Si/Al ratio, it was found that at lower Si/Al ratio of zeolite L, the adsorption capacity was enhance due to more compensated by K+ ions, so that there are more sites for ethylene adsorption [29]. Based on this reason, it was anticipated that the first group could better adsorb ethylene than the other one.

Table 2. Textural properties of different morphologies of zeolite L crystals.

Gel composition K_2O:Al_2O_3:SiO_2:H_2O	**Morphology**	**Surface Area (m^2/g)**	**External surface Area (m^2/g)**	**Micropore surface area (m^2/g)**	**Total pore volume (cm^2/g)**	**Si/Al ratio**
2.62 : 1 : 8 : 160	Ice hockey	327.3	33.46	293.8	0.2319	3.30
3.54 : 1 : 10 : 160	Clam	320.1	22.48	297.7	0.1457	3.40
2.62 : 1 : 10 : 100	Disk	324.9	15.27	309.7	0.1775	3.70
2.62 : 1.2 : 10 : 160	Short cylindrical	247.9	16.88	231.1	0.2027	3.80
2.62 : 1 :10 : 160	Long cylindrical	232.3	14.20	218.1	0.1480	3.70

4. Conclusion

Well crystalline zeolite L could be synthesized with different mole ratios of aK_2O: bAl_2O_3: $cSiO_2$: dH_2O and it appeared with different morphologies and crystal sizes. The optimal molar compositions to yield a

pure phase of highly crystalline zeolite L in different shapes were $2.62K_2O$: Al_2O_3: $10SiO_2$: $160H_2O$ for a long cylindrical shape, $2.62K_2O$: 1.2 Al_2O_3: $10SiO_2$: $160H_2O$ for a short cylindrical shape, $2.62K_2O$: Al_2O_3: $10SiO_2$: $80H_2O$ for a round shape, $3.54K_2O$: Al_2O_3: $10SiO_2$: $160H_2O$ for a clam shape and $2.62K_2O$: Al_2O_3: $8SiO_2$: 160 H_2O or $3.04K_2O$: Al_2O_3: $10SiO_2$: 160 H_2O for an ice hockey shape. The differences in crystal sizes and shapes of the resulting zeolite L caused by nucleation and crystal growth which depended strongly on starting gel compositions and crystallization condition. The change in morphology seemed related to the crystal sizes. The faster the nucleation/crystallization occurred, the smaller crystal sizes were achieved. The results of characterization as well as the adsorption of ethylene indicated that the crystal morphologies and also the crystal sizes affected the physicochemical properties of zeolite L.

References

[1] J. M. Newsam, "Structures of dehydrated potassium zeolite L at 298 and 78K and at 78K containing sorbed perdeuteriobenzene," *Journal of Physical Chemistry A*, vol. 93, pp. 7689, 1989.

[2] D. W. Breck, *Zeolite Molecular Sieves: Structure, Chemistry and Use*. New York: Wiley, 1974, pp. 113-156.

[3] C. S. Carr and D. F. Shantz, "Synthesis of high aspect ratio low-silica zeolite L rods in oil/water/surfactant mixtures," *Chemistry of Materials*, vol. 17, pp. 6192-6197, 2005.

[4] Y. S. Ko and W. S. Ahn, "Crystallization of zeolite L from Na_2O–K_2O–Al_2O_3–SiO_2–H_2O system," *Powder Technology*, vol. 145, pp. 10-19, 2004.

[5] Y.-J. Lee, J. S. Lee, and K. B. Yoon, "Synthesis of long zeolite-L crystals with flat facets," *Microporous and Mesoporous Materials*, vol. 80, pp. 237-246, 2005.

[6] S. D. Bhat, P. S. Niphadkar, T. R. Gaydhankar, S. V. Awate, A. A.Belhekar, and P. N. Joshi, "High temperature hydrothermal crystallization, morphology and yield control of zeolite type K-LTL," *Microporous and Mesoporous Materials*, vol. 76, pp. 81, 2004.

[7] A. Z. Ruiz, D. Brühwiler, T. Ban, and G. Calzaferri, "Synthesis of zeolite L tuning size and morphology," *Monatshefte für Chemie,* vol. 136, pp. 77-89, 2005.

[8] T. Ban, H. SaitO, M. Naito, Y. Ohya, and Y. Takahashi, "Synthesis of zeolite L crystals with different shapes," *Journal of Porous Materials,* vol. 14, pp. 119-126, 2007.

[9] O. Larlus and V. P. Valtchev, "Crystal morphology control of LTL-type zeolite crystals," *Chemistry of Materials,* vol. 16, pp. 3381, 2004.

[10] G. Calzaferri, O. Bossart, D. Brühwiler, S. Huber, C. Leiggener, K. M. van Veen, and A. Z. Ruiz, "Light-harvesting host–guest antenna materials for quantum solar energy conversion devices," *Comptes Rendus Chimie,* vol. 9, pp. 214-225, 2006.

[11] S. Trakarnroek, S. Jongpatiwut, T. Rirksomboon, S. Osuwan, and D. E. Resasco, "N-octane aromatization over Pt/KL of varying morphology and channel lengths," *Applied Catalysis A: General,* vol. 313, pp. 189-199, 2006.

[12] G. Peiser and T. V. Suslow, "Factors affecting ethylene adsorption by zeolite: The last word (from us)," *Perishables Handling Quart*, vol. 95, pp. 17-19, 1998.

[13] H. Zhao, G. F. Vance, G. K. Ganjegunte, and M. A. Urynowicz, "Use of zeolites for treating natural gas co-produced waters in Wyoming, USA," *Desalination*, vol. 228, pp. 263-276, 2008.

[14] A. van Miltenburg, W. Zhu, F. Kapteijn, and J. A. Moulijn, "Adsorptive separation of light olefin/paraffin mixture," *Chemical Engineering Research and Design*, vol. 84, pp. 350-354, 2006.

[15] N. Patdhanagul, T. Srithanratana, K. Rangsriwatananon, and S. Hengrasmee, "Ethylene adsorption on cationic surfactant modified zeolite NaY." *Microporous and Mesoporous Materials*, vol. 131, pp. 97-102, 2010.

[16] E. Costa, G. Calleja, A. Jimenez, and J. Pau, "Adsorption equilibrium of ethylene, propane, propylene, carbon dioxide, and their mixtures on 13X zeolite," *Journal of Chemical & Engineering Data*, vol. 36, no. 2, pp. 218-224, 1991.

[17] N. Sue-aok, T. Srithanratana, K. Rangsriwatananon, and S. Hengrasmee, "Study of ethylene adsorption on zeolite NaY modified with group I metal ions," *Applied Surface Science*, vol. 256, pp. 3997-4002, 2010.

[18] D. J. C. Yates, "On the location of adsorbed ethylene in a zeolite," *Journal of Physical Chemistry*, vol. 70, pp. 3693-3697, 1966.

[19] J. P. Verduijn, "Zeolite L," U.S. Patent 5 242 675, Sept. 7, 1993.

[20] M. M. J. Treacy, J. B. Higgins, and R. Von Ballmons, *Collection of simulated XRD power diffraction pattern of zeolites*. Elsevier, 2001.

[21] Y. S. Ko and W. S. Ahn, "Synthesis and characterization of zeolite L," *Bulletin of the Korean Chemical Society,* vol. 20, 1999.
[22] M. A. Ali, B. Brisdon, and W. J. Thomas, "Synthesis, characterization and catalytic activity of ZSM-5 zeolites having variable silicon-to-aluminum ratios," *Applied Catalysis A: General,* vol. 252, pp. 149-162, 2003.
[23] Y. J. Wu, X. Q. Ren, Y. D. Lu and J. Wang, "Crystallization and morphology of zeolite MCM-22 influenced by various conditions in the static hydrothermal synthesis," *Microporous and Mesoporous Materials,* vol. 112, pp. 138-146, 2008.
[24] Y. C. Kim, J. Y. Jeong, J. Y. Hwang, S. D. Kim, and W. J. Kim, "Influencing factors on rapid crystallization of high silica nano-sized zeolite Y without organic template under atmospheric pressure," *Journal of Porous Materials*, vol. 16, pp. 299-306, 2009.
[25] A. Sagarzazu and G. González, "Aluminum content on the crystallization of zeolite beta," *Microscopy and Microanalysis*, vol. 11, pp. 1560-1561, 2005.
[26] Y. S. Ko and W. S. Ahn, "Influence of synthesis parameters on the morphology and particle size distribution of zeolite L," *Journal of Industrial and Engineering Chemistry*, vol. 10, pp. 636-644, 2004.
[27] P. K. Bajpai, M. S. Rao, and K. V. G. K. Gokhale, "Synthesis of mordenite type zeolites," *Industrial & Engineering Chemistry Product Research and Development*, vol. 17, pp. 223, 1978.
[28] R. Brent and M. W. Anderson, "Fundamental crystal growth mechanism in zeolite L revealed by atomic force microscopy," *Angewandte Chemie International Edition,* vol. 47, pp. 5327-5330, 2008.
[29] G. Calleja, J. Pau, and J. A. Calles, "Pure and multicomponent adsorption equilibrium of carbon dioxide, ethylene, and propane on ZSM-5 zeolites with different Si/Al ratios," *Journal of Chemical & Engineering Data*, vol. 43, pp. 994-1003, 1998.